Published in final edited form as:
J Photochem Photobiol A Chem. 2008 December 15; 200(2-3): 438–444. doi:10.1016/j.jphotochem.2008.09.008.

Fluorescence lifetime properties of near-infrared cyanine dyes in relation to their structures

Hyeran Lee[a], **Mikhail Y. Berezin**[a], **Maged Henary**[b], **Lucjan Strekowski**[b], and **Samuel Achilefu**[a]

[a] Department of Radiology, Washington University, St Louis, MO 63110, U.S.A. Fax: 314-747-5191; Tel: 314-362-8599; E-mail: achilefus@mir.wustl.edu

[b] Department of Chemistry, Georgia State University, Atlanta, GA 30302-4098, U.S.A.

Abstract

Structurally diverse near-infrared (NIR) absorbing polymethine dyes were prepared and their fluorescence lifetimes (FLT) were evaluated in relation to their structural features. Comparative FLT analysis based on the modification of methine chain length and heterocyclic system showed that indolium or benz[*e*]indolium heptamethine dyes exhibited longer FLT than the benz[*c*,*d*]indolium trimethine dye. Modification of heterocyclic system alone with an intact chain length showed that indolium-based heptamethine dyes showed approximately 30% longer FLT than the benz[*e*] indolium-based dyes. In general, the FLT of polymethine dyes increased from polar to non-polar solvents. In addition, correlation study between the theoretical and the experimental FLT for indocyanine green (ICG) suggests that the lack of structural rigidity for these cyanine dyes is primarily responsible for the loss of the excited state energy via non-radiative pathway.

Keywords

Cyanine dyes; Fluorescence lifetime

1. Introduction

Steady-state fluorescence technique is frequently applied in biomedical research because of its high sensitivity and ease of data acquisition. However, time-resolved fluorescence measurements are advantageous for interrogating molecular and physiological processes within a fluorophore's local environment compared to the steady-state data [1]. The intricate balance between the high sensitivity of the fluorescence lifetime (FLT) properties of organic dyes to their mediums and the independence of FLT on the local dye concentration or photobleaching is a compelling reason for using FLT measurements in heterogeneous mediums such as cells and tissues. The importance of FLT in analytical chemistry was recently demonstrated by a concerted effort by world leaders to establish FLT standards for organic dyes using both time- and frequency-domain time-resolved fluorescence measurements [2]. Whereas all the dyes used in that study absorb and fluoresce in the UV/vis region where tissue autofluorescence interfere with detection sensitivity, the heightened interest in the use of near-

Correspondence to: Samuel Achilefu.

infrared (NIR) fluorescent dyes (λ_{max} 700–900 nm) for in-cellular and in vivo imaging studies motivated us to evaluate the FLT of NIR fluorescent polymethine dyes. This class of dyes are particularly used in a variety of biological applications because of their excellent spectral properties and biocompatibility [3–5].

Much attention has focused on the photophysical properties of cyanine dyes including their absorption and emission spectra, fluorescence quantum yields, and FLTs. Different approaches have been attempted to improve the overall photophysical properties of cyanine dyes. As shown in Fig. 1, there are four major decay pathways from the excited singlet state to the ground state ($S_1 \rightarrow S_0$) for these dyes. These are fluorescence (k_{fl}) radiative process and three non-radiative pathways consisting of internal conversion (k_{ic}), intersystem crossing to form a triplet state (k_{isc}), and photoisomerization or torsional rotation to form cis-cyanine (k_{rot}) [6,7].

A previous study suggested that torsional rotation about one of the carbon-carbon methine bonds accounts for ca. 90% of the first excited singlet state decay through a radiationless pathway [6]. Internal conversion is the second major pathway and the intersystem crossing pathway was suggested to be insignificant. Although theoretical premise on the first excited singlet state pathways of cyanine dyes have been examined extensively, the experimental FLT data often contradicts the theoretical prediction, making it difficult to estimate the FLT accurately. Therefore, experimentally determined FLTs of these NIR dyes are important for adequate characterization and a full realization of the utility of time-resolved measurements in biomedical research. Here, we report the synthesis and photophysical properties of structurally diverse NIR polymethine cyanine dyes primarily focusing on the effects of structural changes on their FLTs.

2. Experimental

2.1 Materials

IR-820 and ICG were purchased from commercial sources and were used without further purification. All solvents used for optical measurements were spectroscopic grade.

For spectroscopy study, dyes were dissolved in 150 μL of DMSO as stock solutions. To prevent inner effect in fluorescent measurement, aliquots (10 μL) were diluted until the absorbance was ≤ 0.15. In some cases, the samples were dissolved at higher concentrations in dichloromethane and chloroform to obtain a measurable signal for fluorescence lifetime measurements.

2.2 Methods

^{1}H NMR spectra were recorded on Omega GE at 300 MHz at room temperature in DMSO-d_6 and referenced to tetramethylsilane (TMS) as an internal standard. The steady-state absorption and emission spectra were recorded on a Beckman Coulter DU 640 UV-VIS spectrophotometer and Fluorolog III fluorimeter (Horiba Jobin Yvon), respectively. Fluorescence lifetime was measured using a time-correlated single photon counting (TCSPC) technique (Horiba, Kyoto, Japan) with excitation source NanoLed at 773 nm (Horiba) and impulse repetition rate of 1 MHz at 90° to a R928P detector (Hamamatsu Photonics, Hamamatsu City, Japan). The detector was set to 820 nm with a 20 nm band pass. The electrical signal was amplified by a TB-02 pulse amplifier (Horiba), and the amplified signal was fed to the constant fraction discriminator (CFD) (Philips, Eindhoven, The Netherlands). The first detected photon represented the start signal by the time-to-amplitude converter (TAC), and the excitation pulse triggered the stop signal. The multichannel analyzer (MCA) recorded repetitive start-stop signals from the TAC and generated a histogram of photons as a function of time-calibrated channels (6.88 ps/channel) until the peak signal reached 10,000 counts. The lifetime was recorded on a 50 ns scale. The instrument response function was obtained by using

Rayleigh scatter of Ludox-40 (Sigma-Aldrich, St. Louis, MO) (0.03% in Millipore quality water) in a quartz cuvette at 773 nm emission. DAS6 v6.1 decay analysis software (Horiba) was used for lifetime caculations. The goodness of fit was judged by χ^2 values and Durbin-Watson parameters and visual observations of fitted line, residuals, and autocorrelation function.

2.3 Preparation of fluorescence lifetime probes

2.3.1. Heptamethine cyanine dyes 2, 3 and 6 (Figure 2)—Syntheses of these dyes were carried out using the reported procedure [8].

*Dye **2***. Yield, 60%; ^{1}H NMR: δ 1.00 (s, 12H), 1.64 (m, 10H), 1.87 (m, 4H), 2.62 (m, 4H), 4.03 (m, 4H), 6.18 (br d, J = 14 Hz, 2H), 6.92 (br d, J = 14 Hz, 2H), 7.06 (t, J = 7 Hz, 2H), 7.26 (m, 4H), 7.34 (d, J = 7 Hz, 2H), 7.39 (d, J = 8 Hz, 2H), 8.08 (d, J = 8 Hz, 2H). λ_{max} (in MeOH): 760 nm (ε 180,000 $M^{-1}cm^{-1}$). ESI-MS *m/z*: 812 ([M^+-Na], 100).

*Dye **3***. Yield, 73%; ^{1}H NMR: δ 1.77 (m, 10H), 2.54 (m, 4H), 2.68 (m, 4H), 4.43 (m, 4H), 6.55 (br d, J = 14 Hz, 2H), 7.36 (t, J = 8 Hz, 2H), 7.53 (t, J = 8 Hz, 2H), 7.78 (br d, J = 14 Hz, 2H), 7.80 (d, J = 8 Hz, 2H), 7.87 (d, J = 8 Hz, 2H), 7.95 (d, J = 8 Hz, 2H), 8.05 (d, J = 8 Hz, 2H). λ_{max} (in MeOH): 795 nm (ε 110,000 $M^{-1}cm^{-1}$). ESI-MS *m/z*: 793 ([M^+-Na], 100).

*Dye **6***. Yield, 98%; ^{1}H NMR: δ 1.36 (s, 12H), 1.73 (m, 8H), 2.57 (t, J = 7 Hz, 4H), 3.06 (m, 4H), 4.15 (m, 4H), 6.20 (br d, J = 12 Hz, 2H), 7.19 (m, 2H), 7.39 (m, 6H), 7.48 (d, J = 7 Hz, 2H), 7.55 (d, J = 7 Hz, 2H), 8.18 (d, J = 8 Hz, 2H). λ_{max} (in MeOH): 795 nm (ε 210,000 $M^{-1}cm^{-1}$). ESI-MS *m/z*: 799 ([M^+-Na], 100).

2.3.2 Pentamethine cyanine dye 8 (Scheme 1)—A mixture of **7** (50 mg, 0.18 mmol) and malonaldehyde dianil hydrochloride (25 mg, 0.09 mmol) heated under reflux in EtOH in the presence of sodium acetate (23 mg, 0.28 mmol) for 72 h. The reaction mixture was cooled to room temperature and ether was added to the crude mixture to precipitate solid. The crude product was then filtered off, washed with ether and recrystallized from methanol/ether to give the desired dye **8**. Yield, 65%. λ_{max} (in MeOH): 815 nm. ESI-MS *m/z*: 595 ([M^+-Na], 100).

2.3.3 Trimethine cyanine dye 15 (Scheme 2)—Benz[c,d]indole-2(1H)-thione **10** [9,[10]], 2-methylthiobenz[*c,d*]indole hydroiodide **11** [9,[11]], and 2-(2,2-dimethyl-4,6-dioxo-1,3-dioxane-5-yliden)1*H*-benz[*c,d*]indole **12** [9,[12]] were prepared by using the reported procedures.

2.3.3.1. Ethyl 2-(2,2-dimethyl-4,6-dioxo-1,3-dioxan-5-ylidene)-1H-benz[c,d]indole-1-hexanoate (13): A mixture of compound **12** (3 g, 10.2 mmol), ethyl 6-bromohexanoate (5.5 g, 30.6 mmol) and K_2CO_3 (4.2 g, 30.60 mmol) were heated in DMF (40 mL) at 90 °C for 18 h under a nitrogen atmosphere. The mixture was cooled to room temperature and filtered. The filtrate was concentrated under reduced pressure. The residue was purified on silica gel (flash chromatography, EtOAc-hexane, 1:2) providing 3g (6.86 mmol, 67%) of **13** as a red solid; mp 142–143 °C; ^{1}H NMR λ δ 1.11 (t, J = 8.0 Hz, 3H), 1.20–1.30 (m, 2H), 1.40–1.53 (m, 2H), 1.74 (s, 6 H), 1.79–1.87 (m, 2H), 2.22 (t, J = 8.3 Hz, 2H), 3.97 (q, J = 8.0 Hz 2H), 4.34 (t, J = 8.3 Hz, 2H), 7.77 (t, J = 8.3 Hz, 1H), 7.73 (t, J = 8.7 Hz, 1H), 7.99–8.06 (m, 2H), 8.43 (d, J = 8.7 Hz, 1H), 8.90 (d, J = 8.0 Hz, 1H); ^{13}C NMR δ 14.5, 24.4, 26.1, 26.8, 28.5, 33.7, 48.8, 60.1, 81.7, 102.4, 115.3, 123.8, 126.5, 129.1, 129.3, 130.4, 131.5, 134.7, 134.8, 140.4, 162.4, 165.1, 173.1; MS (70 eV) m/z 438 ([M^++1], 100); ESI-HRMS calcd. for $C_{25}H_{28}NO_6$ (M^++1) 438.1917, found 438.1921.

2.3.3.2. 1-(5-Carboxypentyl)-2-methylbenz[c,d]indolium iodide (14): Ester **13** (1 g, 2.9 mmol) was dissolved in acetic acid (4 mL) and the mixture was refluxed for 20 min.

Concentrated HCl (4 mL) was added dropwise to the refluxing mixture until the color changed from red to green. The mixture was cooled to room temperature, and saturated KI solution was added until the product started to precipitate. The product was filtered off, washed with ether, crystallized from methanol, and dried in vacuo affording 1 g (2.4 mmol, 83%); mp 218 °C (dec.); ^{1}H NMR δ 1.34–1.59 (m, 4H), 1.89–1.96 (m, 2H), 2.22 (t, J = 8.0 Hz, 2H), 3.25 (s, 3H), 4.67 (t, J = 8.0 Hz, 2H), 8.02 (t, J = 8.7 Hz, 1H), 8.18 (t, J = 8.3 Hz, 1H), 8.46 (d, J = 8.7 Hz, 1H), 8.56 (d, J = 8.0 Hz, 1H), 8.82 (d, J = 8.7 Hz, 1H), 8.98 (d, J = 8.0 Hz, 1H); ^{13}C NMR δ 15.03, 24.49, 26.14, 29.51, 33.91, 47.29, 115.12, 121.69, 122.41, 128.62, 129.61, 130.20, 131.38, 135.73, 138.92, 139.10, 173.07, 174.93; MALDI-MS m/z 282 ([M^+-I], 100); ESI-HRMS calcd for $C_{18}H_{20}NO_2$ (M^+-I) 282.1494, found 282.1497.

2.3.3.3 Trimethine cyanine dye (15): Analogous to the reported procedure[13], a mixture of compound **14** (15 mg, 0.037 mmol) and ethyl orthoformate (0.1 ml, 0.60 mmol) were stirred in pyridine (2 ml) at room temperature for 48 h. The reaction progress was monitored by visible/near-infrared spectroscopy and LC-MS for aliquots diluted with methanol until compound **14** disappears. The reaction mixture was then purified by reverse phase column chromatography (Biotage SP4 purification system) eluting the compound with water/acetonitrile to give **15** as a green solid. Yield, 51%; ^{1}H NMR δ (m, 8H), 1.87 (m, 4H), 2.23 (t, J = 7 Hz, 4H), 4.39 (m, 4H), 7.25 (br d, J = 13 Hz, 2H), 7.79 (t, J = 8 Hz, 2H), 7.88 (d, J = 8 Hz, 2H), 8.06 (t, J = 8 Hz, 2H), 8.36 (d, J = 8 Hz, 2H), 8.58 (m, 4H), 9.19 (t, J = 13 Hz, 1H), 12.01 (s, 2H). λ_{max} (in MeOH): 760 nm (ε 107,000 $M^{-1}cm^{-1}$). ESI-MS m/z: 573 ([M^+-I], 100).

3. Results and Discussion

3.1 Synthesis of structually diverse NIR fluorescent dyes

As the importance of NIR fluorescent cyanine dyes in biological imaging continues to increase, dyes with distinctive structural features are developed to optimize desired spectral properties. Specifically, the heterocyclic bases and the polymethine chain that connects these heterocyclic bases generally determine their optical properties. Creating structurally diverse NIR fluorescent molecules while maintaining their light absorption and emission properties between 700 and 900 nm range requires a careful choice of both heterocyclic and polymethine fluorophore groups. First, we investigated the correlation between the methine chain length and the FLT by comparing hepta-, penta-, and tri-methine dyes. Our lab and other have developed diverse NIR fluorescent heptamethine dyes for biological imaging[8,[14],[15]]. Structures of the heptamethine dyes under investigation are shown in Figs. 2 and 3. Detailed syntheses of the dyes are either described elsewhere (dyes **1**, **4**, **5** [8,[15]] or carried out using a similar procedure (dyes **2**, **3**, **6**). For clarity, these dyes were broadly divided into two groups based on their heterocyclic ring systems.

In the above examples, the spectral properties of the heptamethine dyes remained in the desired NIR range for both benz[*e*]indolium (Fig. 2) and indolium (Fig.3) derivatives. Unfortunately, the sole modification of methine chain from heptamethine to either pentamethine or trimethine with an intact indolium or benz[*e*]indolium heterocyclic system would result in absorption maxima shift into the visible region. To overcome this problem, different heterocyclic systems were needed. Literature reports show that replacement of benz[*e*]indolium with quinolinium- or benz[*c*,*d*]indolium-based heterocyclic systems results in bathochromic shifts of about 100 or 200 nm, respectively, and that each additional methine group contributes about 100 nm bathochromic shift to the polymethine cyanine dyes. Consequently, pentamethine and trimethine NIR cyanine dyes could be prepared with quinolinium or benz[*c*,*d*]indolium heterocyclic systems.

Quinolinium-based NIR pentamethine dye was prepared by condensation of **7** with malonaldehyde dianil hydrochloride as shown in Scheme 1. The reaction progressed slowly and the formation of **8** required a continuous heating of **7** for 72 h. The absorption and emission maxima of **8** are 815 and 830 nm, respectively.

Synthetic pathway to NIR trimethine dye is rather lengthy and involved 6 steps as shown in Scheme 2. The key step is the formation of 5-(benz[*c,d*]indol-1*H*-2-ylidene)-1,3-dioxane-4,6-dione **12** [12], the alkylation of which provides an easy access to a variety of 1-alkyl-substituted 2-methylbenz[*c,d*]indolium salts. These salts are important precursors to different carbocyanine dyes. Benz[*c,d*]indole derivatives **10**–**12** were synthesized as previously described [9–11] starting with the commercial substrate **9**.

Compound **12** was allowed to react with ethyl 6-bromohexanoate under basic conditions to afford an ester **13**, which was then transformed into a quaternary salt **14**. Compound 14 was purified by crystallization from methanol. The condensation of **14** with ethyl orthoformate furnished the benz[*c,d*]indolium trimethine cyanine dye **15**.

3.2 Spectroscopic characteristics of structurally diverse NIR fluorescent cyanine dyes

The spectral and FLT properties of the NIR dyes used in this study are summarized in Table 1. The FLT of ICG was determined to be 0.97 ns in DMSO (Fig. 2, Table 1). Substitution of *N*-alkylsulfonato functionality of ICG with *N*-alkylcarboxy moiety to give cypate [16,17] resulted in a marginal FLT decreased to 0.87 ns. Rigidifying chromophore systems in organic molecules is an established strategy to stabilize fluorescent dyes and optimize their photophysical properties, including fluorescence quantum yields and FLTs [18]. Literature reports have demonstrated that incorporating a cyclohexene ring in the polymethine chain minimizes non-radiative decay via trans-cis isomerisation, thereby increasing the quantum yield and the FLT [19,20]. Accordingly, we incorporated a 6-membered ring system into the linear polymethine chain in anticipation of increasing the FLT of the dyes. To further reduce the heavy-atom effect, we substituted meso-chlorine atom with a phenyl group using a published procedure.[8] Although the fluorescence quantum yield of heptamethine dye **1** with reinforced meso-substituted aromatic group improved compared to the linear polymethine dye ICG, the FLTs of both compounds did not change. However, substitution of the meso-chloro group in IR-820 with the phenylcarboxy group to give **1** increased the FLT from 0.48 ns to 0.98 ns in DMSO. Interestingly, the FLT of a meso-bromo substituted analogue of IR-820 dye was determined to be 0.58 ns (structure not shown). This finding is in contrast to the typical observations that intramolecular heavy atom perturbs the singlet excited state by facilitating intersystem crossing into the triplet state [21–23]. As a result, the bromo-substituted dye was expected to have shorter FLT than the chloro-substituted analogue. Previous report by Soper *et al* [24] also showed that FLTs of these organic dyes increased with increasing molecular weight of the intramolecular heavy-atom modifications, with concomitant FLT increase in the order F < Cl < Br < I. They also demonstrated that the heavy-atom modification did increase the efficiency of crossing into the triplet state, with the heavier atom showing a larger rate of intersystem crossing. Thus, our results suggest that heavy atom-mediated intersystem crossing and other factors determine the FLTs of these dyes.

Having established the FLT properties of the heptamethine dyes using benz[*e*]indolium heterocyclic system (Fig. 2), we evaluated the FLTs of indolium-based heptamethine cyanine dyes (Figure 3, Table 1). Although the absorption and emission maxima of indolium dyes decreased by about 35 nm and 30 nm, respectively, relative to the benz[e]indolium analogue (see **1** and **2**), these spectral properties were retained in the desired NIR range. A remarkable FLT increase from 0.98 ns for **1** to 1.48 ns for **2** was observed. The overall results show that indolium-based dyes generally exhibit approximately 30% longer FLTs relative to the structurally similar benz[*e*]indolium dyes. Murphy *et al* [6] suggested that increase in the size

of the heterocyclic system results in FLT increase by possibly retarding $K_{rot.}$ However, our results clearly show that benz[*e*]indolium dyes with the bulky ring system have shorter FLT, suggesting that the extra phenyl group in **1** destabilized the excited state of the NIR dye relative to **2**.

To further assess the effects of different substituent at the C-3 or C-5 positions of indolium moiety on their FLTs, we prepared and analyzed the selenium and thiol derivatives. Substitution of $C(Me)_2$ (**2**) at C-3 position with S (**3**) or Se (**4**) decreased the FLT from 1.48 ns to the respective 1.26 ns and 1.28 ns. This data suggests that the heavy-atom effect plays an important role because substitution of carbon with sulfur or selenium in the ring systems facilitated the intersystem crossing, as previously reported [25]. Other structural changes also affected the FLTs of these dyes. For example, substitution of H at C-5 position of the indolium with sulfonate group (**5**) decreased the FLT from 1.48 to 1.33 ns. In addition, modification of the ring structure at the meso-position of polymethine chain from 6-membered ring (**2**) to 5-membered ring (**6**) decreased the FLT from 1.48 ns to 1.11 ns in DMSO. These data clearly demonstrate the influence of different substituents on heptamethine-based NIR fluorescent cyanine dyes. The heptamethine dyes described above yielded FLTs in DMSO ranging from 0.50 ns to 1.48 ns. This presents a wide scale of FLTs for imaging molecular processes in cells and animals using fluorescence lifetime imaging microscopy or diffuse optical tomography systems with high temporal resolution.

Our next objective was to assess the effects of changing the methine chain length on FLT. For the reasons given above, we prepared the benz[*c*,*d*]indolium trimethine dye **15**. As predicted, we obtained a NIR dye that absorbed and emitted light at 760 nm and 798 nm in DMSO, respectively (Table 1).

The FLT of the newly developed **15** was 0.3 ns whereas those of linear heptamethine dyes were close to 1 ns in DMSO. The dramatic decrease in FLT could be attributed to the influence of both the heterocyclic system and/or the short polymethine chain. Interestingly, previous reports by Kasatani et al. and Petrov et al. showed that the FLT of UV/vis-absorbing trimethine dye, 3,3′-diethylthiacarbocyanine iodide (DTCI), was also 0.299 ns in the same solvent system [26,[27]]. Based on the methine chain length, Kasatani's group also demonstrated that the FLTs of these dyes decreased in the order of pentamethine < heptamethine < trimethine when the chain length was modified without altering the heterocyclic structure. Interestingly, our results show that modification of heterocyclic base from benzothiazole trimethine to benz[*c*,*d*]indole trimethine with intact chain length did not change the FLT. A previous study suggested that the shorter FLT of the trimethine cyanine dye was due to steric hindrance between the heteroaromatic fragments with a short methine chain [7]. This factor partly contributes to the nonradiative decay pathway, which results in the observed FLT decrease. Based on literature reports, we expected the pentamethine cyanine dyes to exhibit longer FLT than either trimethine or heptamethine compounds. Surprisingly, the FLT of pentamethine dye **8** was 0.36 ns in DMSO.

The FLT dependence of these dyes on various solvents was then evaluated to provide insights into the excited state decay pathway. While it is generally accepted that photoisomerization decay pathway (k_{rot}) is solvent dependent and that internal conversion (k_{ic}) is a solvent independent process, it is not clear which of the solvent properties, including viscosity, polarity, or hydrogen bonding has a dominant effect on the decay pathway. To further complicate the problem, several studies on the FLT dependence of cyanine dyes on solvent viscosity have reported contradictory results [7,[26]] Our previous studies showed that cyanine dyes are mostly insensitive to solvent viscosity but highly sensitive to the solvent polarity [28]. Accordingly, we determined the FLTs of these dyes in various solvents with different solvent polarity. Our results showed a large dependence of FLT on the solvent polarity (Table 1). In general, the

FLT increased from the polar solvents to the non-polar solvents in the order water < MeOH < EtOH < acetone < DMSO < DCM < $CHCl_3$, with an average FLT increase of 6–8 folds in $CHCl_3$ compared to water.

To understand the decay pathway for these dyes, we determined the theoretical maximum FLT of ICG based on the theoretical relationship between absorption intensity and FLT. This relationship was derived by Strickler and Berg from Einstein fundamental equation on induced absorption and spontaneous emission. In addition to Einstein formula, Strickler-Berg expression takes into account the frequency difference between absorption and emission [29] as shown below:

$$1/\tau_0 = 2.880 \times 10^{-9} n^2 \langle \tilde{\nu}_f^{-3} \rangle_{Av}^{-1} (g_l/g_u) \int \varepsilon(\nu) d\ln \tilde{\nu}, \mathrm{C}^{-1} \quad (1)$$

where n is a refractive index, $\varepsilon(\nu)$ is the molar absorptivity absorption spectra, $\langle \tilde{\nu}_f^{-3} \rangle_{Av}^{-1} = \tilde{\nu}_f^3$ in cm^{-1} and equivalent for fluorescent maximum for sharp emission, g_l and g_u are the degeneracies of the lower and upper states and equal to $g_1/g_u = 1$ for fluorescence transition.

The above formula is based on several assumptions, one of which is the absolute rigidity of the molecule with no change in geometry. Thus, this approach provides an estimate of possible maximum FLT value of cyanine molecules such as ICG when restricted from any rotations. The calculated theoretical FLT value was 3.5 ns compared to the experimental value of 0.97 ns which is only about 28 % of the theoretical value. These results show that over 70% of the excited state energy is lost through non-radiative pathways due to the lack of structural rigidity for these dyes. Thus, it is evident that the major decay pathway for polymethine cyanine dyes is via non-radiative photoisomerization process or torsional rotation. Our findings suggest that rigidifying the structural framework of cyanine dyes is the best approach to design polymethine cyanine-type molecule with long FLTs. Specifically, minimizing the free rotation of the flanking polymethine chain can increase the FLT of NIR polymethine dyes to the maximum possible theoretical value.

4. Conclusions

Structurally diverse NIR cyanine dyes were prepared, including a new method for the synthesis of benz[*c*,*d*]indolium trimethine dye. The structural relationship of these dyes to their FLTs was evaluated. Overall, heptamethine cyanine dyes exhibited longer FLT compared to the trimethine or pentamethine dyes and indolium-based heptamethine dyes showed longer FLT than the corresponding benz[*e*]indolium counterparts. In addition, the FLTs increased from the polar solvents to the non-polar solvents. Correlation study between the theoretical maximum (3.49 ns) and experimental (0.97 ns) FLTs of ICG shows that the major loss of excited energy (>70%) was by non-radiative pathway, which could be attributed to the lack of structural rigidity for these cyanine dyes.

Acknowledgments

We thank Dr. Yunpeng Ye for synthesizing cypate. This research was supported in part by the National Institutes of Health grants R01 CA109754, and R01 EB1430.

References

1. Reynolds JS, Troy TL, Mayer RH, Thompson AB, Waters DJ, Cornell KK, Snyder PW, Sevick-Muraca EM. Photochem Photobiol 1999;70:87–94. [PubMed: 10420847]

2. Boens N, Qin W, Basaric N, Hofkens J, Ameloot M, Pouget J, Lefevre JP, Valeur B, Gratton E, Vandeven M, Silva ND Jr, Engelborghs Y, Willaert K, Sillen A, Rumbles G, Phillips D, Visser AJ, Hoek A, Lakowicz JR, Malak H, Gryczynski I, Szabo AG, Krajcarski DT, Tamai N, Miura A. Anal Chem 2007;79:2137–2149. [PubMed: 17269654]
3. Ntziachristos V, Yodh AG, Schnall M, Chance B. Proc Natl Acad Sci U S A 2000;97:2767–2772. [PubMed: 10706610]
4. Bloch S, Lesage F, McIntosh L, Gandjbakhche A, Liang K, Achilefu S. J Biomed Opt 2005;10:054003. [PubMed: 16292963]
5. Gurfinkel M, Thompson AB, Ralston W, Troy TL, Moore AL, Moore TA, Gust JD, Tatman D, Reynolds JS, Muggenburg B, Nikula K, Pandey R, Mayer RH, Hawrysz DJ, Sevick-Muraca EM. Photochem Photobiol 2000;72:94–102. [PubMed: 10911733]
6. Murphy S, Schuster GB. J Phys Chem 1995;99:8516–8518.
7. Soper SA, Mattingly QL. J Am Chem Soc 1994;116:3744–3752.
8. Lee H, Mason JC, Achilefu S. J Org Chem 2006;71:7862–7865. [PubMed: 16995699]
9. Ficken GE, Kendall JD. J Chem Soc 1960:1537–1541.
10. Lakshmikantham MV, Chen W, Cava MP. J Org Chem 1989;54:4746–4750.
11. Deligeorgiev TG, Drexhage GNIKH. Dyes Pigm 1991;15:215–223.
12. Vasilenko NP, Mikhailenko FA, Rozhinsky JI. Dyes Pigm 1981;2:231–237.
13. Reddington MV. J Chem Soc, Perkin Trans 1 1998:143–147.
14. Hilderbrand SA, Kelly KA, Weissleder R, Tung CH. Bioconjugate Chemistry 2005;16:1275–1281. [PubMed: 16173808]
15. Lee H, Mason JC, Achilefu S. Journal of Organic Chemistry 2008;73:723–725. [PubMed: 18095702]
16. Ye Y, Li WP, Anderson CJ, Kao J, Nikiforovich GV, Achilefu S. J Am Chem Soc 2003;125:7766–7767. [PubMed: 12822971]
17. Achilefu S, Dorshow RB, Bugaj JE, Rajagopalan R. Invest Radiol 2000;35:479–485. [PubMed: 10946975]
18. Cooper M, Ebner A, Briggs M, Burrows M, Gardner N, Richardson R, West R. J Fluoresc 2004;14:145–150. [PubMed: 15615040]
19. Ozmen B, Akkaya EU. Tetrahedron Lett 2000;41:9185–9188.
20. Grigonis R, Derevyanko NA, Ishchenko AA, Sirutkaitis V. Quantum Electronics 2001;31:1027–1031.
21. Davidson RS, Bonneau R, Joussot-Dubien J, Trethewey KR. Chem Phys Lett 1980;74:318–320.
22. Kavarnos G, Cole G, Scribe P, Dalton JC, Turro NJ. 1971;93:1032–1034.
23. McGlynn, SP.; Azumi, T.; Kinoshita, M. Molecular Spectroscopy of the Triplet State. Englewood Cliffs: NJ Prentice Hall; 1969. Pages
24. Flanagan JH, Owens CV, Romero SE, Waddell E, Kahn SH, Hammer RP, Soper SA. Anal Chem 1998;70:2676–2684. [PubMed: 9666731]
25. Redmond RW, Kochevar IE, Krieg M, Smith G, McGimpsey WG. J Phys Chem A 1997;101:2773–2777.
26. Kasatani K, Sato H. Bull Chem Soc Jpn 1996;69:3455–3460.
27. Petrov NK, Gulakov MN, Alfimov MV, Busse G, Frederichs B, Techert S. J Phys Chem, A 2003;107:6341–6344.
28. Berezin MY, Lee H, Akers W, Nikiforovich G, Achilefu S. Proc SPIE 2008;6867:68670J-68670J-68611.
29. Strickler SJ, Berg RA. J Chem Phys 1962;37:814–822.

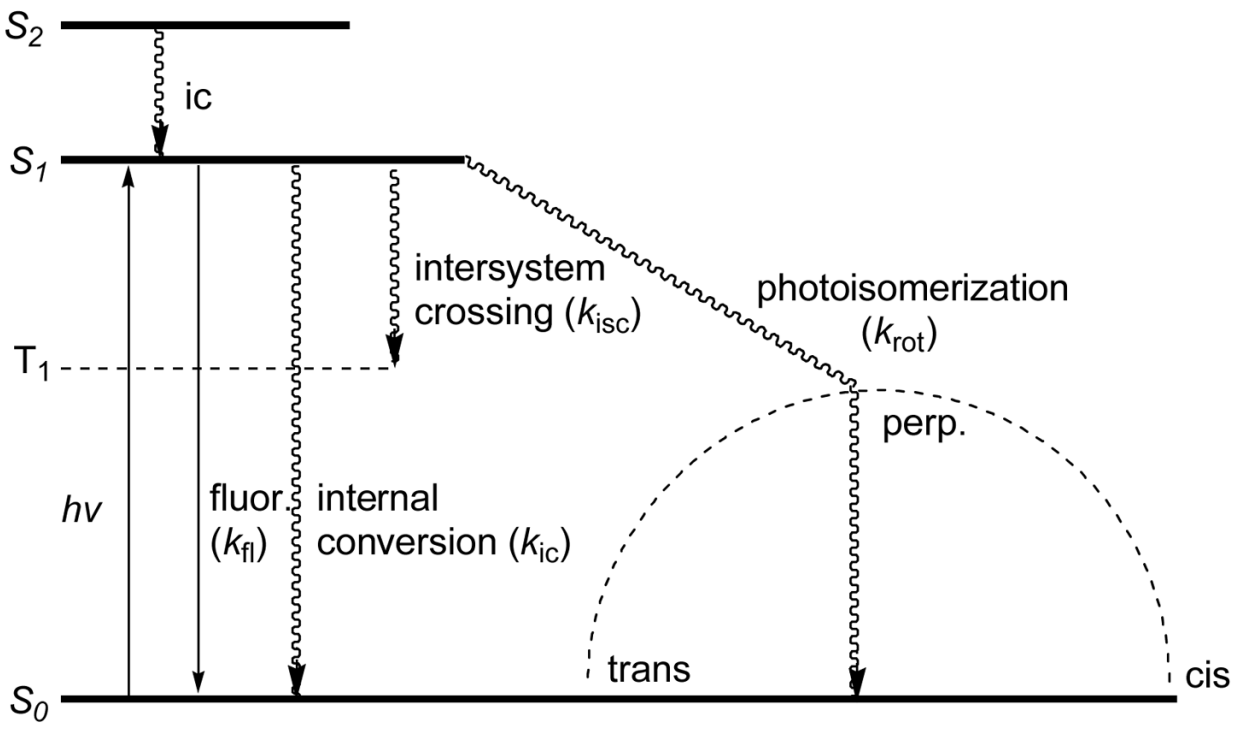

Fig. 1.
Energy level diagram of typical polymethine dyes depicting relaxation processes following the singlet excited state.

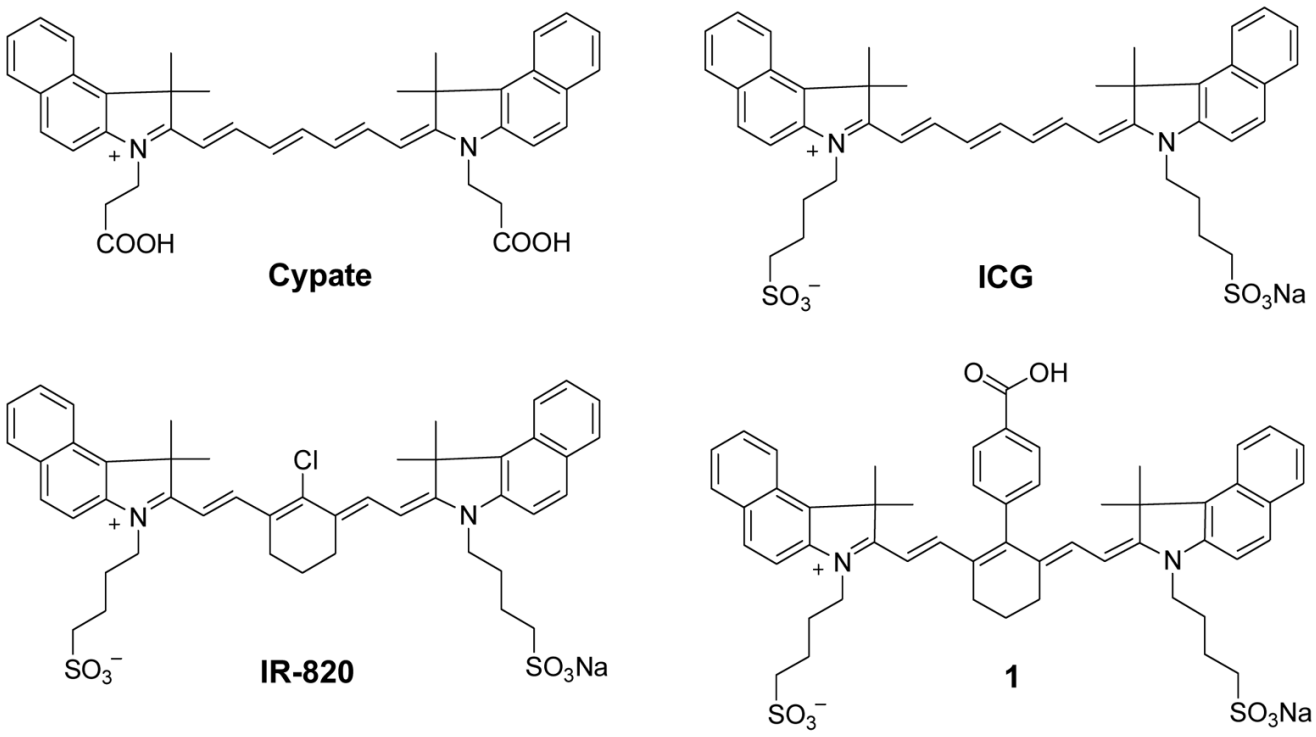

Fig. 2.
Structures of NIR benz[*e*]indolium heptamethine dyes.

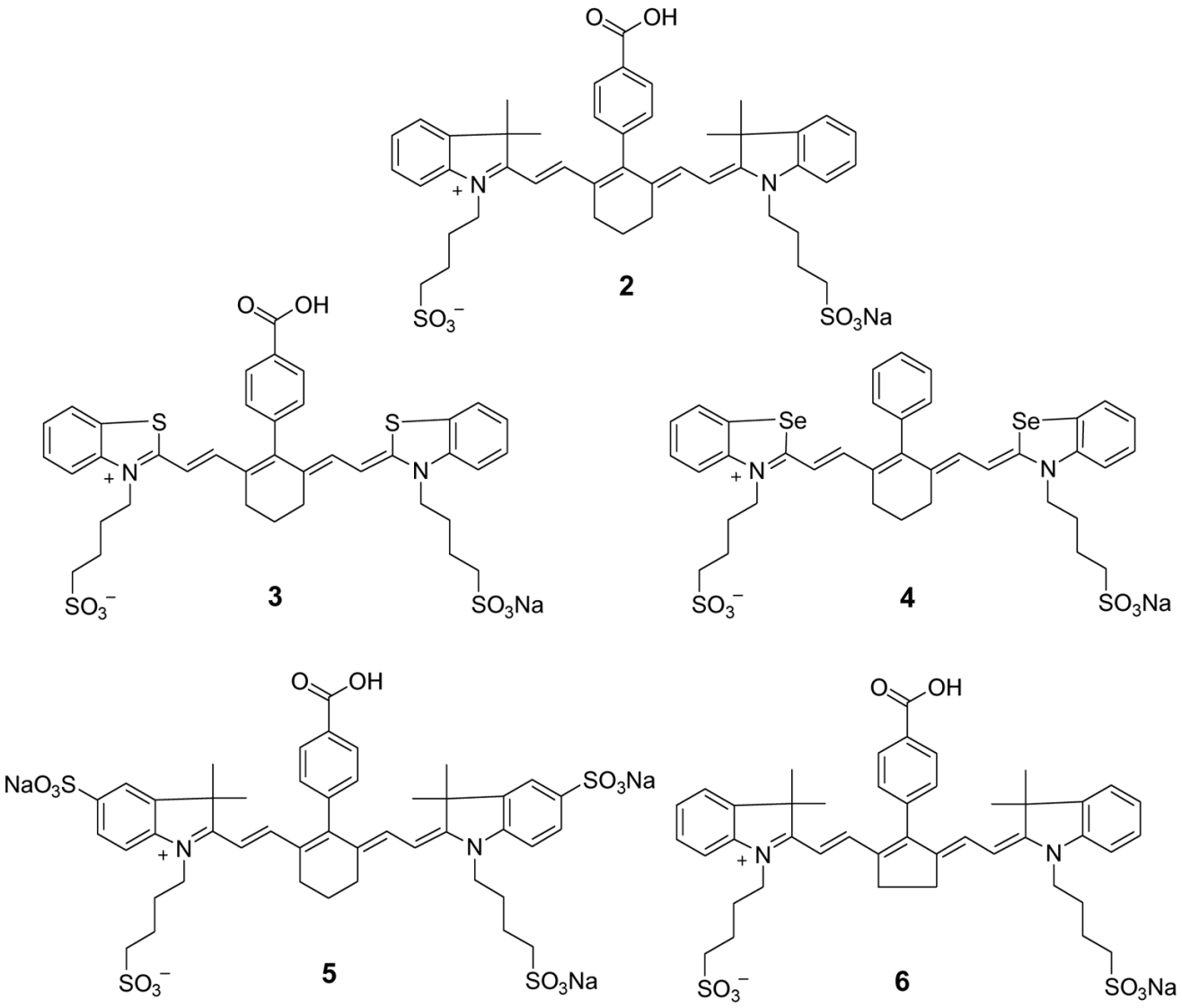

Fig. 3.
Structures of NIR indolium heptamethine dyes.

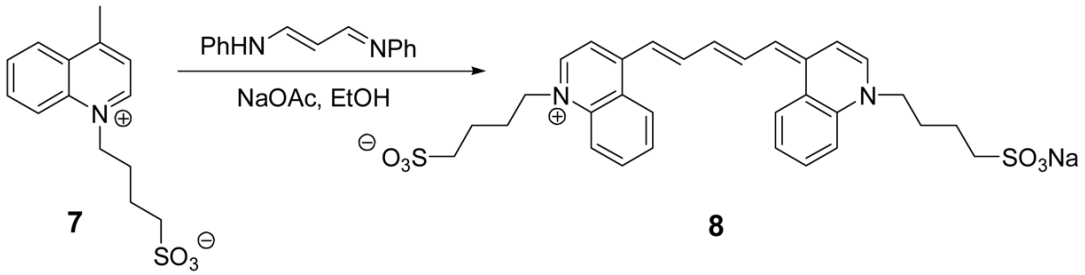

Scheme 1.
Synthesis of quinolinium pentamethine dye **8.**

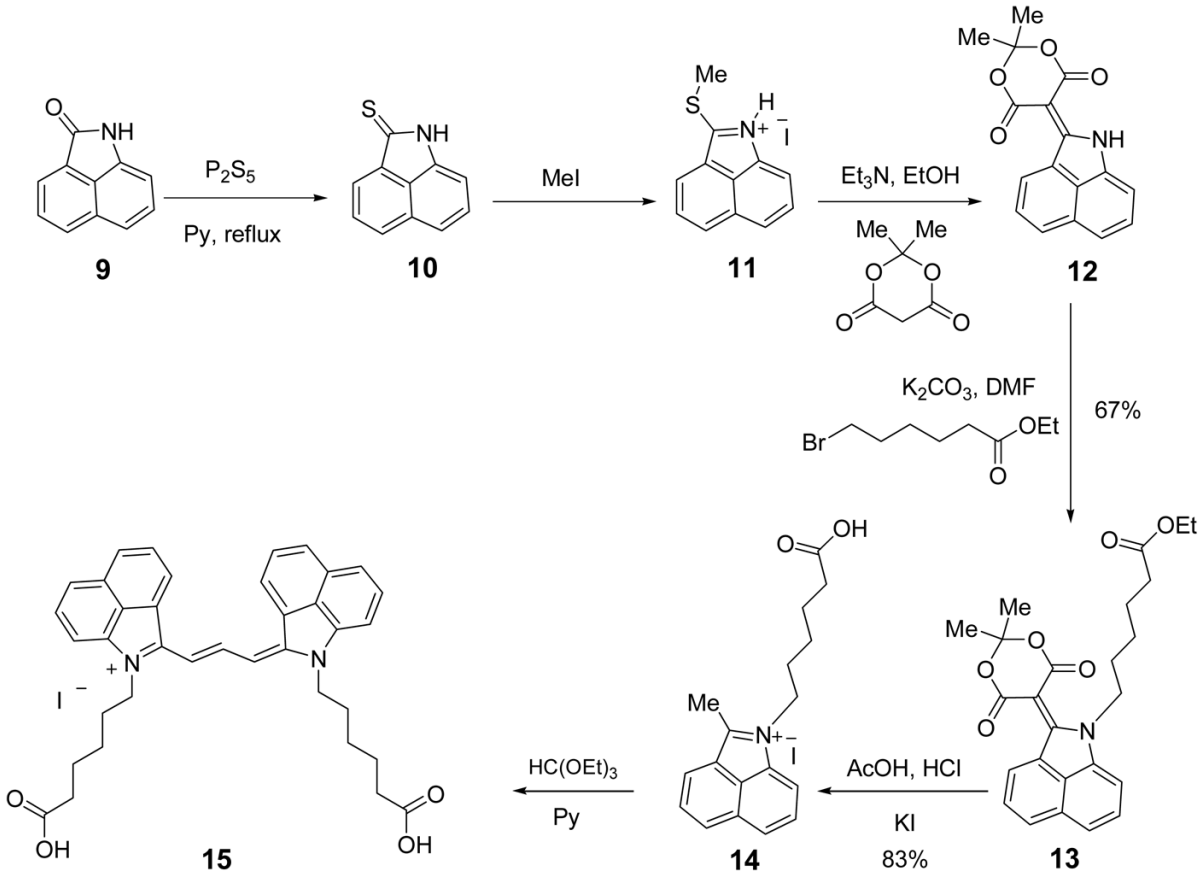

Scheme 2.
Synthesis of benz[*c*,*d*]indolium trimethine dye **15.**

Table 1

Spectroscopic Characteristics of Polymethine Dyes.

		Cypate	ICG	IR-820	1	2	3	4	5	6	8	15
λ_{abs} (nm, methanol)		792	792	820	800	765	800	800	770	797	815	760
λ_{em} (nm, methanol)		817	817	836	811	780	813	813	790	816	830	773
τ_f(ns)	water	0.20	0.17	0.13	0.20	0.44	0.33	0.36	0.44	0.36	n/a	n/a
	methanol	0.46	0.51	0.25	0.61	0.98	0.72	0.73	0.81	0.83	n/a	n/a
	ethanol	0.57	0.62	0.38	0.69	1.25	0.93	0.93	1.00	0.87	n/a	n/a
	acetone	0.80	0.87	0.43	0.84	1.13	1.08	1.14	1.02	1.13	n/a	n/a
	DMSO	**0.87**	**0.97**	**0.50**	**0.98**	**1.48**	**1.26**	**1.28**	**1.33**	**1.11**	**0.36**	**< 0.3**
	dichloromethane	0.94	0.91	0.59	1.34	1.24	1.19	1.29	n/a	1.17	n/a	n/a
	chloroform	1.01	1.14	0.73	1.62	1.30	1.31	1.29	n/a	1.25	n/a	n/a

J Photochem Photobiol A Chem. Author manuscript; available in PMC 2009 December 15.